analytical chemistry

pubs.acs.org/ac Letter

Magnetically Levitated Plasma Proteins

Ali Akbar Ashkarran, Kenneth S. Suslick, and Morteza Mahmoudi*

Cite This: *Anal. Chem.* 2020, 92, 1663−1668 Read Online

ACCESS | Metrics & More | Article Recommendations | Supporting Information

ABSTRACT: Surprisingly, the densities of proteins in solution, which are important fundamental biophysical quantities, have not been accurately measured. The lack of such data can limit meaningful interpretation of physical and chemical features of proteins and enzymes. Here, we demonstrate a new technique using superparamagnetic iron oxide nanoparticles (SPIONs) for magnetic levitation (MagLev), which promises to more precisely measure the density of proteins in solution. As a test of our new technique, we have levitated human plasma proteins using MagLev. By using standard density glass beads for calibration, MagLev showed that the levitated plasma proteins have a measured density in solution of 1.03 ± 0.02 g/cm^3, which is much lower than those reported or assumed in the past literature (i.e., ∼1.35 g/cm^3). Our findings suggest that MagLev may provide useful insights into the measurement of densities for better understanding the solution properties of proteins and their interactions both with other proteins in solution and with solvating water molecules.

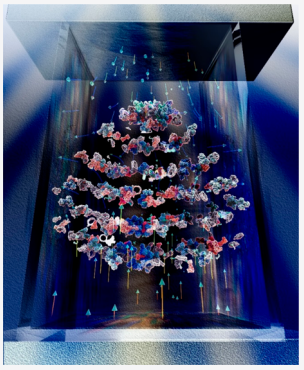

There has been a long-standing and intense debate in the literature regarding the precise density of proteins in solution.[1−4] To date, researchers have been using an average density value estimated as 1.35 g/cm^3 for proteins independent of their nature or molecular weights.[5] This rough density metric can often lead to inaccurate estimates on the other physicochemical and composite protein features,[5] especially after their interactions with other materials such as nanoparticles.[6,7]

Density is a universal physical property specific to each substance.[8] In this regard, density-based separation methods and density measurements have been widely used as analytical tools.[9] A number of methods are available for measuring densities of materials either as solid or liquid states, including chromatography,[10] hydrometry,[11] pycnometry,[12] microchannel resonators,[13] and dielectrophoretic field-flow fractionation.[14] Each of these methods, however, fail in one or more of the critical criteria of high accuracy, repeatability, low cost, ease of operation, or portability.[15]

Compared to the aforementioned approaches, magnetic levitation (MagLev) of diamagnetic or weakly paramagnetic materials in a paramagnetic solution has been shown to provide a promising platform for density measurements. MagLev is accurate, rapid, easy to use, and inexpensive,[16−18] and it has proven to be a robust and highly reproducible technique to solve a broad range of problems in physics, chemistry, engineering, and biology, including analysis of food and water, quality control of materials, diagnosis, kinetics of free-radical polymerization, self-assembly, and separation of materials from mixtures.[19−24] One of the limitations of the Mag-Lev, however, prevents its prior use for determining the density of biomolecules. The time required for levitation closely depends on the size of the diamagnetic materials, a limitation that causes prohibitively long times of separation when the forces or Brownian motion are larger than the coalescing forces of MagLev, especially for objects smaller than ∼2 μm (e.g., essentially all biomolecules).[25]

Equilibration of levitation for micrometer-sized species requires as much as 24 h.[26] Slightly larger objects take less time but are still relatively slow, e.g., about an hour for ∼10 μm objects.[27] This time and size limitation can prevent the practical use of MagLev for many applications (e.g., point of care diagnosis, biological and biochemical substances, and multistep procedures) in which short-time separations of submicrometer objects are essential. The other problem of the use of MagLev in biological/biomedical applications is the toxicity or incompatibility of the current paramagnetic solutions (e.g., $GdCl_3$, $MnCl_2$, and $MnBr_2$) to the biological systems.[28] While such paramagnetic solutions may be compatible with whole organisms or even individual cells, they often lead to denaturation of proteins in solution.

Here, for the first time, we have developed MagLev with the use a biocompatible superparamagnetic solution, the commercially available ferumoxytol (an FDA-approved superparamagnetic iron oxide nanoparticles (SPIONs) suspension), instead of the conventional paramagnetic solutions (e.g., $GdCl_3$, $MnBr_2$, $MnCl_2$, etc.). Our main hypothesis was that the SPIONs are be more compatible with plasma proteins, compared to the common paramagnetic solutions, and also provide a higher magnetic susceptibility for a liquid and

Received: November 8, 2019
Accepted: January 3, 2020
Published: January 9, 2020

https://dx.doi.org/10.1021/acs.analchem.9b05101
Anal. Chem. 2020, 92, 1663−1668

consequently, a much faster separation of proteins in solution.[29] In fact, the magnetization of superparamagnetic materials such as SPIONs is approximately linear with a higher magnetic susceptibility compared with diamagnetic or paramagnetic materials.[30] Applying an external magnetic field attracts the paramagnetic solution toward the area with maximum field strength and pushes the levitating object to the locations with less field strength. Therefore, the object will move from a higher-field to a lower-field region and this effect can be improved by increasing the magnetic field gradient or the susceptibility of the MagLev solution (i.e., SPIONs).[30,31] Indeed, we find that we can reproducibly and reliably levitate plasma proteins and define their densities using MagLev.

EXPERIMENTAL DETAILS

Materials. SPIONs (30 mg/mL) functionalized with ferumoxytol was obtained from Feraheme (www.feraheme.com) and diluted with phosphate buffered saline (PBS 1×, HyClone) solution to 0.25 mg/mL. For all experiments, 100 μL of proteins was pipetted into the glass tube containing SPIONs solution and levitated for 3 h until they reached their equilibrium positions within the MagLev device. After 3 h, no changes in levitation pattern of protein samples were observed.

The MagLev platform (Figure 1) consist of two N42-grade neodymium (NdFeB) cubic magnets (25.4 mm length, 25.4 mm width, and 50.8 mm height) with 2.5 cm separation distance and the N poles facing each other.

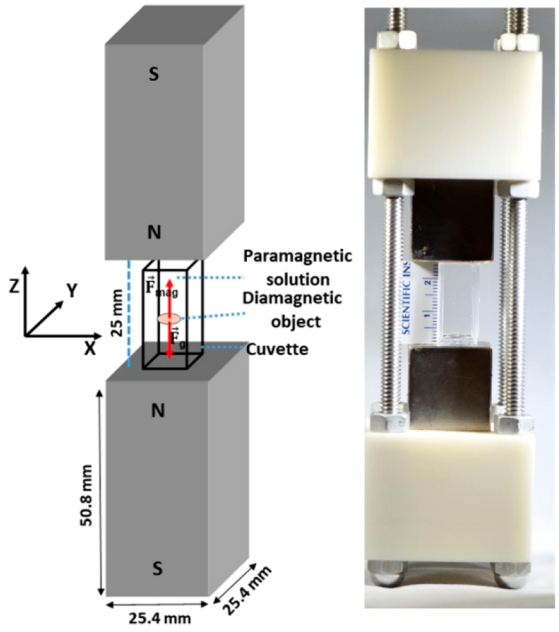

Figure 1. Schematic and the corresponding photograph of the MagLev platform.

Characterization. The cubic NdFeB magnets (grade N42, model no. NB044) were purchased from Magnet4less. Strength of the magnetic field which was measured by a dc gauss meter (vector/magnitude Gauss meter model VGM, Alphalab) was ~0.5 T on the surface of the magnet. Calibrated density standards (±0.0002 g/cm^3 at 23 °C) were obtained from American Density Materials (Stauton, VA; www.americandensitymaterials.com). The optical images and levitation heights of the proteins were imaged using a Nikon D750 (equipped with a 105 mm Nikkor Microlens) digital camera and a ruler with millimeter-scaled marking, respectively. The levitation height was measured with respect to the top surface of the bottom magnets (i.e., $z = 0$) using a millimeter scaled ruler. The levitation height was always the center of the particles/cloud/bands. Therefore, considering the millimeter scaled ruler that was used, the accuracy of levitation height readings was ±1 mm. A 4 mL plastic cuvette which was cut to 2.5 cm was used as a levitation container for MagLev. Standard density fluorescent polyethylene microspheres densities were obtained from Cospheric (www.cospheric.com).

LC−MS/MS Sample Preparation. Proteins were reduced with 10 mM dithiothreitol for 1 h at 56 °C and then alkylated with 55 mM iodoacetamide (Sigma) for 1 h at 25 °C in the dark. Proteins were then digested with modified trypsin (Promega) in 100 mM ammonium bicarbonate, pH 8.9 at 25 °C overnight. Trypsin activity was halted by addition of formic acid (99.9%, Sigma) to a final concentration of 5%. Peptides were desalted using peptide desalting spin columns (Pierce) then vacuum centrifuged. Peptides were loaded on a precolumn and separated by reversed-phase HPLC using an EASY-nLC1000 (Thermo) over a 140 min gradient before nanoelectrospray using a QExactive HF-X mass spectrometer (Thermo). The mass spectrometer was operated in a data-dependent mode. The parameters for the full scan MS were resolution of 70 000 across 350−2000 m/z, AGC 3×10^6, and maximum IT 50 ms. The full MS scan was followed by MS/MS for the top 15 precursor ions in each cycle with a NCE of 28 and dynamic exclusion of 30 s. Raw mass spectral data files (.raw) were searched using Proteome Discoverer 2.2 (Thermo) and Mascot version 2.4.1 (Matrix Science). Mascot search parameters were 10 ppm mass tolerance for precursor ions, 15 mmu for fragment ion mass tolerance, 2 missed cleavages of trypsin, fixed modification was carbamidomethylation of cysteine, and variable modifications were methionine oxidation. Only peptides with a Mascot score greater than or equal to 25 and an isolation interference less than or equal to 30 were included in the data analysis.

Mathematical Derivations. By solving Maxwell's equations, we can obtain an approximation for the B (x, y, z) field, between two magnets in the absence of the paramagnetic medium. In an anti-Helmholtz configuration, the behavior of magnetic field between two magnets is given by[24]

$$\vec{B} = \begin{pmatrix} B_x \\ B_y \\ B_z \end{pmatrix} = \begin{pmatrix} 0 \\ 0 \\ \frac{-2B_0}{d}z + B_0 \end{pmatrix} \quad (1)$$

The components of the B-field in the XY plane cancel out each other, and we only have a B-field in the z direction (Figure S6):

$$B_z = B_0 - \frac{2B_0 Z}{d}, \begin{cases} Z = 0 \rightarrow B = B_0 \\ Z = \frac{d}{2} \rightarrow B = 0 \\ Z = d \rightarrow B = -B_0 \end{cases} \quad (2)$$

A diamagnetic sample levitates in the MagLev device when the gravitational force acting on the sample is balanced by the magnetic force produced through the paramagnetic medium due to the external applied magnetic field (eq 5).[27]

https://dx.doi.org/10.1021/acs.analchem.9b05101
Anal. Chem. 2020, 92, 1663−1668

$$\vec{F}_{mag} = \frac{(\chi_s - \chi_m)}{\mu_0} V(\vec{B} \cdot \vec{\nabla})\vec{B} \quad (3)$$

$$\vec{F}_g = (\rho_s - \rho_m)V\vec{g} \quad (4)$$

$$\vec{F}_{mag} + \vec{F}_g = 0 \quad (5)$$

During the levitation, these two forces are balanced, and we obtain

$$\frac{(\chi_s - \chi_m)}{\mu_0}\left(B_x\frac{\partial B_z}{\partial x} + B_y\frac{\partial B_z}{\partial y} + B_z\frac{\partial B_z}{\partial z}\right) - (\rho_s - \rho_m)g = 0 \quad (6)$$

Using eq 1 in eq 6, we have[26]

$$\rho_s = \alpha h + \beta \quad (7)$$

$$\alpha = \frac{4(\chi_s - \chi_m){B_0}^2}{g\mu_0 d^2} \quad (8)$$

$$\beta = \rho_m - \frac{2(\chi_s - \chi_m){B_0}^2}{g\mu_0 d} \quad (9)$$

Equation 7 clearly indicates a linear relationship between the levitation height of a diamagnetic object and its density in a paramagnetic solution within the MagLev platform.

RESULTS AND DISCUSSION

To levitate human plasma proteins in the system, we first used a conventional $GdCl_3$ solution (0.25 M) to probe the density of the plasma proteins in the MagLev platforms that we developed in-house for this study (Figure 1).

Not surprisingly, the plasma proteins became denatured and sedimented in the $GdCl_3$ solution, probably due to interactions with the high concentration of gadolinium complex ions[32] (Figure S1 of Supporting Information). To solve this problem, next we used the commercially available biocompatible Gadovist (GV), which has a chelated structure, in order to protect gadolinium ions and reduce toxicity. However, the GV was unable to levitate the plasma proteins at concentrations lower than 2 M. Furthermore, the same protein denaturation issue reoccurred but at longer levitation times (sedimentation starts after ~15 min in 0.5 M and lower concentrations of GV) (Figure S1). In addition, the solubility of the $GdCl_3$ in PBS is considerably lower than in pure water (solubility images are shown in Figure S2 of the Supporting Information).

Given that proteins are not stable in the gadolinium-containing paramagnetic solutions, we then used a suspension of SPIONs for the MagLev medium. In addition to their biocompatibility, the SPION suspensions have higher magnetic susceptibilities (due to their superparamagnetic properties), which allows faster separation of nanoscale objects.[33−36] Our results revealed that the levitation process of plasma proteins starts a few minutes after injection of the proteins into the MagLev system and reaches full equilibration within over 3 h (Figure S3).

After adding plasma proteins to SPION solutions in the MagLev setups, we noticed the formation of "ellipsoidal" protein patterns in the MagLev system (Figure 2 and Figure S3 of the Supporting Information). These observed patterns from levitated plasma proteins are highly reproducible. We have investigated the levitation patterns of plasma proteins obtained from different plasma donors (see Movie S1 as representative for a typical formation of ellipsoidal patterns of plasma protein in the MagLev platform). The plasma protein patterns formed were reproducible in all samples, although the concentration of plasma proteins could affect the intensity of the patterns when photographed (Figure S4 of the Supporting Information).

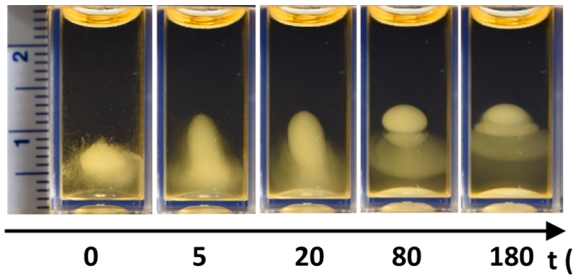

Figure 2. Formation of ellipsoidal patterns from levitated plasma proteins over time, in MagLev platform and 0.06 mg/mL concentration of SPIONs.

Each levitated plasma proteins' pattern consists of several different bands; we could change the dimension of each band and the gap between two individual bands by changing the concentration of SPIONs solution (see Figure S5 of the Supporting Information).

To calibrate the system, we have used commercially available standard density glass beads. A conventional MagLev system consists of two coaxial square magnets with like poles facing each other with a separation distance of "d". We consider the z axis as a symmetry axis of the system, where for the upper surface of the bottom magnet $z = 0$ and for the lower surface of the top magnet $z = d$.

The relationship between the levitation height of a diamagnetic object (protein) and its density in a paramagnetic solution within the MagLev platform can be derived when the gravitational force acting on the sample is balanced by the magnetic force produced through the paramagnetic medium due to the external applied magnetic field (eq 5).[9] By solving eq 6 (see Figure S6 and details of all calculations and derivations in eqs 1−9 of the Experimental Details section), the equilibrium height of proteins along the glass container can be calculated as[26]

$$h = \frac{(\rho_s - \rho_m)g\mu_0 d^2}{(\chi_s - \chi_m)4{B_0}^2} + \frac{d}{2} \quad (10)$$

In this equation, ρ_m and ρ_s (kg/m^3) are the density of the paramagnetic medium and sample, respectively, g (m/s^2) is the gravitational acceleration, μ_0 (T m A^{-1}) is the permeability of free space, d (m) is the distance between the magnets, B_0 (tesla) is the magnitude of the magnetic field at the surface of the magnets, and χ_m and χ_s (unitless) are the magnetic susceptibilities of the paramagnetic medium and the sample, respectively.

We used standard density glass beads with various densities ranging from 0.9500 g/cm^3 to 1.7500 g/cm^3 for calibration of MagLev device and plotted the standard curves (Figure S7). Levitation of standard density beads revealed that the height profile of particles linearly depends on the density of the standard particles in all three different MagLev systems.

The calibration curve permits the measurement of the absolute density of unknown materials in the MagLev system.

https://dx.doi.org/10.1021/acs.analchem.9b05101
Anal. Chem. 2020, 92, 1663−1668

Considering the calibration curve and levitation height of the protein samples, we may conclude that the density of proteins is 1.03 ± 0.02 g/cm^3. In addition to the standard density beads, we have used three standard fluorescent polyethylene microspheres with known densities (1.011 g/cm^3, 1.033 g/cm^3, and 1.050 g/cm^3) to further confirm the density range of the levitated protein samples, shown in Figure 3. By comparing the

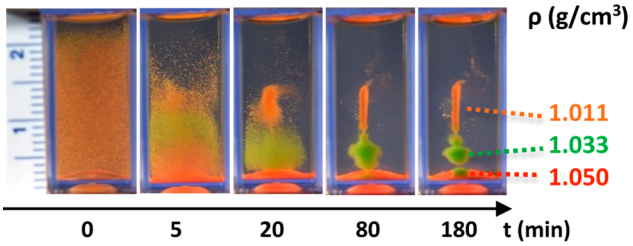

Figure 3. Verification tests via levitating patterns of standard fluorescent polyethylene microspheres over time at 0.06 mg/mL concentration of SPIONs in the MagLev platform. The densities of the orange, green, and red polyethylene microspheres are 1.011 g/cm^3, 1.033 g/cm^3, and 1.050 g/cm^3, respectively.

levitation patterns of fluorescent polymer microspheres in the three different MagLev platforms and the same concentrations as that used for levitation of proteins (0.06 mg/mL), we calculated the density of the plasma proteins. A simple comparison among the levitation heights of the density standard microspheres and the protein samples revealed that the density value of the plasma proteins should be in the range of $1.011 \leq \rho_p$ (g/cm^3) ≤ 1.050, which is much lower than the commonly reported density values of proteins in the literature (i.e., 1.35 g/cm^3).[5]

Fischer and co-workers reported that the average density of proteins versus their molecular weight is not constant as often assumed.[5] For proteins with a molecular weight below 20 kDa, the average density exhibits a positive deviation that increases for decreasing molecular weights.[5] Therefore, we hypothesized that various bands of the levitated plasma proteins should contain proteins with different molecular weights; more specifically, the lower bands of the ellipsoidal levitated plasma proteins should have higher densities (or lower molecular weights) compared to the upper bands. In order to test this hypothesis, we gently collected the six successive bands of solution from top to bottom using a 0.5 mL syringe under a constant controlled negative pressure (see Figure S8 for a detailed step-by-step procedure of a typical band extraction in the MagLev system). The extracted bands were analyzed by SDS-PAGE, as demonstrated in Figure S9. The outcome revealed that there were differences (at least in band densities) in the protein profiles of various bands from top to bottom; the gel outcomes also indicated a limited correlation between the molecular weights of proteins and small changes in their densities. To further analyze the types and concentration of the participated plasma proteins in each band, we also performed liquid chromatography−mass spectroscopy (LC−MS/MS) on the bands and the outcomes were in line with the SDS-PAGE results (Figure S10 and Excel file S1 of the Supporting Information). Calculation of the average density of protein mixtures in each band demonstrated poor correlation between the molecular weights of proteins and small changes in their densities.

It was supposed that the dependency of the density of proteins to their molecular weight is due to the existence of a structured water layer on the surface of the proteins.[5] To further investigate our findings on the limitations in the correlation between the molecular weights of proteins and their densities, we next probed the levitation profiles of ladder proteins, which contains standard proteins with various known molecular weights. Interestingly it was found that the ellipsoidal patterns also appear in levitation profiles of ladder proteins (even more quickly, e.g., after ∼40 min, Figure 4 and Figure S11 of the Supporting Information).

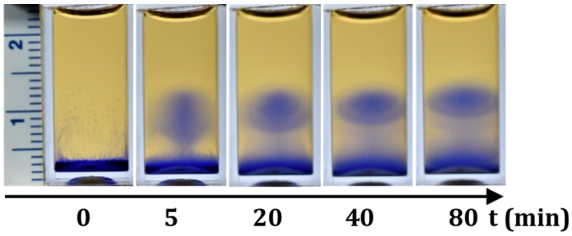

Figure 4. Levitation profiles of precision-plus protein standards (10-protein ladder ranging in molecular mass from 9 to 250 kDa) in MagLev (0.06 mg/mL concentration of SPIONs) over time. It is noteworthy that we used a white background in this experiment to achieve a better color contrast due to the blue color of the ladder.

The SDS-PAGE outcomes of the extracted top, middle, and bottom bands of the levitated ladder proteins demonstrated existence of proteins in the bands regardless of their molecular weights (Figure S12 of Supporting Information). Therefore, levitation patterns in addition to the SDS-PAGE results of standard proteins further suggests that density of the protein cannot be as completely a molecular-weight-dependent function as has been believed previously.[5] To ensure about the SDS-PAGE outcomes, we analyzed the protein types and concentration using LC−MS/MS and the outcomes were in line with the SDS-PAGE results (Figure S13 and Excel file S2 of the Supporting Information).

In addition to human plasma protein samples and the ladder proteins, we levitated a mixture of the three different single protein samples (purchased from Sigma-Aldrich with low (i.e., lysozyme, Mw ∼ 14.4 kDa), middle (i.e., albumin, Mw ∼ 66.4 kDa), and high molecular weight (i.e., immunoglobulin G (IgG), Mw ∼ 150 kDa) ranges in the presence of five standard fluorescent polyethylene microspheres with known densities (1.011 g/cm^3, 1.033 g/cm^3, 1.050 g/cm^3, 1.070 g/cm^3, 1.26 g/cm^3) in the MagLev system at a 0.06 mg/mL concentration of SPIONs. As expected, the outcomes demonstrated that these three different single proteins had the same levitation positions, reindicating that the density of protein is not strictly a molecular-weight-dependent function (Figure 5 and Figure S14).

The levitations profiles of a mixture of single protein samples and standard density fluorescent polyethylene microspheres (Figure S14) over time clearly reveals that the long-assumed density value of protein (i.e., 1.35 g/cm^3) is not correct; again, the levitation heights of all protein solution samples lies in the region of 1.03 g/cm^3 to 1.05 g/cm^3.

The widely used density of 1.35 g/cm^3 was originally deduced from hydrodynamic and adiabatic compressibility experiments.[5] Reanalyzing this traditional approach to density measurements, however, Andersson and Hovmöller[1] chal-

https://dx.doi.org/10.1021/acs.analchem.9b05101
Anal. Chem. 2020, 92, 1663−1668

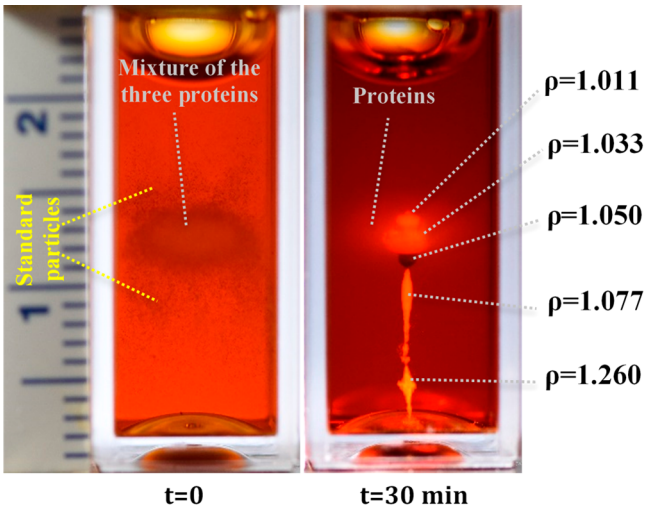

Figure 5. Levitation profiles of three mixed different molecular weights of single proteins (lysozyme, albumin, and immunoglobulin G (IgG)) mixed with five standard density (all density units are g/cm^3) fluorescent polyethylene microspheres in the MagLev system (1 mg/mL concentration of SPIONs). It is noteworthy that the color change is due to the employed higher concentration of SPIONs compared to the other figures.

lenged that the widely used average density value, because of inherent errors in the measurements.[2] They theoretically determined the mass density of a number of proteins using the Voronoi construction (the minimal-sized polyhedron around each atom) and suggested an average density of 1.22 g/cm^3. The Voronoi polyhedron allocates the space within a structure, including cavities or defects, to its constituent atoms to calculate the density.[1,5] The obtained density value in this model was lower than the previously accepted one (1.22 vs 1.35 g/cm^3)[5] but remains significantly higher than the values we have obtained in this study using various MagLev platforms.

CONCLUSIONS

Using superparamagnetic solutions (e.g., SPIONs), instead of paramagnetic solutions, may enable MagLev to levitate a wide range of biomolecules in solution in a reasonable period of time (i.e., a few hours) and, therefore, may pave a way for development of additional biomedical applications including point of care diagnosis and quality assurance testing of macromolecules. Our study on density of protein molecules in solution revealed that the density of plasma proteins in solution is not exclusively a function of molecular-weight. Furthermore, we found that density of plasma proteins in solution has a constant value of 1.03 ± 0.02 g/cm^3 which is significantly lower than that commonly assumed in the literature (i.e., ∼1.35 g/cm^3). Further studies should be conducted to better understand the exact mechanism behind the formation of levitated multiple ellipsoidal plasma patterns. We hypothesize that the multiple ellipsoids may be the outcome of (i) configurational or structural variation of individual proteins or (ii) protein−protein interactions that generate lesser or greater density solution constructs.

ASSOCIATED CONTENT

Supporting Information

The Supporting Information is available free of charge at https://pubs.acs.org/doi/10.1021/acs.analchem.9b05101.

Levitation patterns of human plasma proteins, photographs of samples in DI water, photographs of levitation profiles of human plasma protein samples formation and the formation of ellipsoidal patterns from levitated plasma proteins in MagLev, levitation schematic of magnetic field lines in the MagLev system, calibration curves, typical extraction process of protein bands in the MagLev system, SDS-PAGE analysis, and LC−MS/MS outcomes (PDF)

Full list of identified proteins and their concentration in each band from Figure S10 (XLSX)

Full list of identified proteins and their concentration in each band from Figure S13 (XLSX)

Video representing a typical formation of ellipsoidal patterns of plasma protein in the MagLev platform (AVI)

AUTHOR INFORMATION

Corresponding Author

Morteza Mahmoudi − *Michigan State University, East Lansing, Michigan;* orcid.org/0000-0002-2575-9684; Email: mahmou22@msu.edu

Other Authors

Ali Akbar Ashkarran − *Michigan State University, East Lansing, Michigan*

Kenneth S. Suslick − *University of Illinois at Urbana−Champaign, Urbana, Illinois;* orcid.org/0000-0001-5422-0701

Complete contact information is available at: https://pubs.acs.org/10.1021/acs.analchem.9b05101

Notes

The authors declare no competing financial interest.

ACKNOWLEDGMENTS

This work was supported by the Precision Health Program at Michigan State University.

REFERENCES

(1) Quillin, M. L.; Matthews, B. W. *Acta Crystallogr., Sect. D: Biol. Crystallogr.* **2000**, *D56*, 791−794.
(2) Andersson, K. M.; Hovmoller, S. *Z. Kristallogr. - Cryst. Mater.* **1998**, *213*, 369−373.
(3) Leung, A. K. W.; Park, M. M. V.; Borhani, D. W. *J. Appl. Crystallogr.* **1999**, *32*, 1006−1009.
(4) Tsai, J.; Taylor, R.; Chothia, C.; Gerstein, M. *J. Mol. Biol.* **1999**, *290*, 253−266.
(5) Fischer, H.; Polikarpov, I.; Craievich, A. F. *Protein Sci.* **2004**, *13*, 2825−2828.
(6) Monopoli, M. P.; Walczyk, D.; Campbell, A.; Elia, G.; Lynch, I.; Baldelli Bombelli, F.; Dawson, K. A. *J. Am. Chem. Soc.* **2011**, *133*, 2525−2534.
(7) Walczyk, D.; Bombelli, F. B.; Monopoli, M. P.; Lynch, I.; Dawson, K. A. *J. Am. Chem. Soc.* **2010**, *132*, 5761−5768.
(8) Turker, E.; Arslan-Yildiz, A. *ACS Biomater. Sci. Eng.* **2018**, *4*, 787−799.
(9) Ge, S.; Whitesides, G. M. *Anal. Chem.* **2018**, *90*, 12239−12245.

(10) Baker, L. R.; Stark, M. A.; Orton, A. W.; Horn, B. A.; Goates, S. R. *J. Chromatogr. A* **2009**, *1216*, 5588−5593.
(11) Heinonen, M.; Sillanp, S. *Meas. Sci. Technol.* **2003**, *14*, 625−628.
(12) Stange, U.; Scherf-Clavel, M.; Gieseler, H. *J. Pharm. Sci.* **2013**, *102*, 4087−4099.
(13) Bryan, A. K.; Hecht, V. C.; Shen, W.; Payer, K.; Grover, W. H.; Manalis, S. R. *Lab Chip* **2014**, *14*, 569−576.
(14) Gascoyne, P. R. C. *Anal. Chem.* **2009**, *81*, 8878−8885.
(15) Benz, L.; Cesafsky, K. E.; Le, T.; Park, A.; Malicky, D. *J. Chem. Educ.* **2012**, *89*, 776−779.
(16) Lockett, M. R.; Mirica, K. A.; Mace, C. R.; Blackledge, R. D.; Whitesides, G. M. *J. Forensic Sci.* **2013**, *58*, 40−45.
(17) Nemiroski, A.; Kumar, A. A.; Soh, S.; Harburg, D. V.; Yu, H. D.; Whitesides, G. M. *Anal. Chem.* **2016**, *88*, 2666−2674.
(18) Nemiroski, A.; Soh, S.; Kwok, S. W.; Yu, H. D.; Whitesides, G. M. *J. Am. Chem. Soc.* **2016**, *138*, 1252−1257.
(19) Ge, S.; Semenov, S. N.; Nagarkar, A. A.; Milette, J.; Christodouleas, D. C.; Yuan, L.; Whitesides, G. M. *J. Am. Chem. Soc.* **2017**, *139*, 18688−18697.
(20) Hennek, J. W.; Nemiroski, A.; Subramaniam, A. B.; Bwambok, D. K.; Yang, D.; Harburg, D. V.; Tricard, S.; Ellerbee, A. K.; Whitesides, G. M. *Adv. Mater.* **2015**, *27*, 1587−1592.
(21) Ilievski, F.; Mirica, K. A.; Ellerbee, A. K.; Whitesides, G. M. *Soft Matter* **2011**, *7*, 9113−9118.
(22) Mirica, K. A.; Ilievski, F.; Ellerbee, A. K.; Shevkoplyas, S. S.; Whitesides, G. M. *Adv. Mater.* **2011**, *23*, 4134−4140.
(23) Mirica, K. A.; Phillips, S. T.; MacE, C. R.; Whitesides, G. M. *J. Agric. Food Chem.* **2010**, *58*, 6565−6569.
(24) Subramaniam, A. B.; Yang, D.; Yu, H. D.; Nemiroski, A.; Tricard, S.; Ellerbee, A. K.; Soh, S.; Whitesides, G. M. *Proc. Natl. Acad. Sci. U. S. A.* **2014**, *111*, 12980−12985.
(25) Erickson, H. P. *Biol. Proced. Online* **2009**, *11*, 32−51.
(26) GE, S.; Nemiroski, A.; Mirica, k. A.; Mace, C. R.; Hennek, J. W.; Kumar, A. A.; Whitesides, G. M. *Angew. Chem., Int. Ed.* **2019**, DOI: 10.1002/anie.201903391.
(27) Mirica, K. A.; Shevkoplyas, S. S.; Phillips, S. T.; Gupta, M.; Whitesides, G. M. *J. Am. Chem. Soc.* **2009**, *131*, 10049−10058.
(28) Durmus, N. G.; Tekin, H. C.; Guven, S.; Sridhar, K.; Arslan Yildiz, A.; Calibasi, G.; Ghiran, I.; Davis, R. W.; Steinmetz, L. M.; Demirci, U. *Proc. Natl. Acad. Sci. U. S. A.* **2015**, *112*, E3661−E3668.
(29) Wahajuddin; Arora, S. *Int. J. Nanomed.* **2012**, *7*, 3445−3471.
(30) Gao, Q. H.; Zhang, W. M.; Zou, H. X.; Li, W. B.; Yan, H.; Peng, Z. K.; Meng, G. *Mater. Horiz.* **2019**, *6*, 1359.
(31) Zhao, W.; Cheng, R.; Miller, J. R.; Mao, L. *Adv. Funct. Mater.* **2016**, *26*, 3916−3932.
(32) Jha, S. K.; Marqusee, S. *Proc. Natl. Acad. Sci. U. S. A.* **2014**, *111* (13), 4856−4861.
(33) Laurent, S.; Dutz, S.; Häfeli, U. O.; Mahmoudi, M. *Adv. Colloid Interface Sci.* **2011**, *166*, 8−23.
(34) Mahmoudi, M.; Hofmann, H.; Rothen-Rutishauser, B.; Petri-Fink, A. *Chem. Rev.* **2012**, *112* (4), 2323−2338.
(35) Mahmoudi, M.; Sant, S.; Wang, B.; Laurent, S.; Sen, T. *Adv. Drug Delivery Rev.* **2011**, *63* (1−2), 24−46.
(36) Sharifi, S.; Behzadi, S.; Laurent, S.; Laird Forrest, M.; Stroeve, P.; Mahmoudi, M. *Chem. Soc. Rev.* **2012**, *41* (6), 2323−2343.

https://dx.doi.org/10.1021/acs.analchem.9b05101
Anal. Chem. 2020, 92, 1663−1668